

## RESPONSE OF HELICOPTER BLADES TO A SHARP COLLECTIVE INCREASE

Y. Hecht\* and O. Rand\*\*  
 Faculty of Aerospace Engineering  
 Technion - Israel Institute of Technology  
 Haifa 32000, Israel

## Abstract

The paper presents a theoretical investigation of the response of helicopter blades to a sharp collective increase in hover. The modeling deals with both main aspects of the problem: the spanwise distribution of the unsteady loads, and the corresponding structural dynamic response of the elastic blades and the rotor-fuselage system as a whole. The aerodynamic loads distribution is calculated by the definition and determination of the spanwise distribution of the aerodynamic equivalent mass, which is responsible for the time dependent development of the velocity induced by the trailing vortices. The structural modeling is based on the finite-element approach, and the equations of motion are derived using Lagrange's equations. Due to the sharp changes in time, all terms containing time derivatives are retained in the equations which results in highly nonlinear expressions. A comprehensive investigation was performed to identify and quantify the role and the sensitivity of a variety of parameters. One conclusion is that for high command rates, the induced velocity exhibits relatively slow response and, therefore, the dynamic phenomena become predominant.

## Introduction

One of the maneuvers required in a typical mission of a modern attack helicopter is a "bob-up" climbing from hover in order to be located in minimal time in an upper position. Such a maneuver is achieved mainly by a rapid increase of the collective pitch angle. The helicopter response in this case is complex, and comprehensive analysis is required in order to enable suitable design of rotor systems that will be capable of sustaining sharp loading changes which are forced by the rapid collective increase.

The problem of predicting the aerodynamic loads in the case of a sharp collective change may be viewed as a special case of the general problem of predicting the aerodynamic loads on helicopter blades. In principle, any time stepping numerical scheme (such as those which are based on the vortex theory - see Ref. 1), may be employed for calculating the loads' development due to a sharp collective change (e.g. Ref. 2). It is beyond the scope of this

paper to review the wide range of methods developed for predicting blades' aerodynamic loads and therefore, the following discussion concentrates on the specific case of the loads that result from a sharp collective increase in hover, which exhibits some unique characteristics. Moreover, since the structural and the dynamic analyses of elastic blades require a large number of repeated aerodynamic loads calculations, there is a need to adopt an approximate formulation for the loads prediction. Thus, the discussion will concentrate on such approximate models, while a detailed review of the literature may be found in Ref. [3].

Before preceding to the description of the relevant studies, it should be mentioned that apparently, in hover, rapid collective increase is similar to gust loading (e.g. Ref. 4). However, careful examination shows that these problems are different from both aerodynamic and structural dynamic points of view. In both cases the effective angle of attack grows rapidly, however, in the case of gust loading, the wake vortices are also pushed down by the gust, while in the case of rapid collective pitch increase, the vortices downwards motion is developed gradually by the high intensity vortices that are added to the flowfield after the loads over the blades become higher. From a structural dynamics point of view, the product of inertia which is generated by the pitch angle is absent in gust loading, and therefore, the dynamic couplings are reduced in such cases.

The earliest published investigation of the response of helicopter rotor blades to a rapid collective pitch increase is that of Carpenter and Fridovich [5]. In this report, experimental data of blades undergoing sharp collective changes up to 200/sec. are presented along with correlation with an analytical model. The latter was based on the apparent mass of the air associated with the acceleration of an impervious disc normal to its plane, and includes some correction constants. The dynamic analysis is based on the assumption that the blades were infinitely stiff. This work served as a basis for comparison of advanced models reported in Refs. [6, 7].

Rebont et al. [6] presented an experimental investigation for the case of descending axial flight and correlated the results with theoretical predictions based on a model similar to the one presented in Ref. [5]. They concluded that a double value for the apparent mass yields better agreement

---

\*Graduate Student

\*\*Senior Lecturer

with experimental results in this case.

Pitt and Peters [7] proposed the model known as "dynamic inflow" which is based on analytic solution of the flow-field around the rotor disc while the pressure distribution is described by a special family of known functions. This model relates the aerodynamic perturbation in thrust, roll moment and pitch moment to the induced flow distribution by a linear first order system of equations. For the axial flight region, it has been concluded that the apparent mass terms for the simplest pressure distribution are identical to those obtained for an impermeable disc, but these values vary significantly with the pressure distribution. It has been also recommended to develop a dynamic inflow model that will account also for wake contraction, finite number of blades and reduced frequency effects.

Chen and Hindson [8] reviewed the influence of dynamic inflow on the helicopter vertical response. They compared the models presented in Refs. [5] and [7], and concluded that there is reasonable agreement between calculated results of these models and experiments, and that the induced velocity and initial conditions play an important role. They also indicated that the model presented in Ref. [7] tends to produce more oscillatory response, and that taking into account the changes in the rotor speed may improve the correlation.

One of the earliest numerical, time-stepping schemes that was used for simulating the case of a sharp collective change is the model of Segal [2] who utilized a detailed wake modeling based on the vortex theory. However, the calculated results of this analysis include no distinction between the aerodynamic thrust and the total thrust which will be discussed later.

Reference [9] presents a recent identification study of the rotor/fuselage system vertical response in hover. The modeling includes three degrees of freedom, the inflow, the coning and heaving motion. The paper stresses the need to incorporate a real wake influence and blade flexibility effects.

Generally, the above investigations show that unsteady aerodynamic response (which may be expressed in terms of dynamic inflow response) plays an important role, and that allowing rotor speed variations may improve the results' quality. However, it should be emphasized, that the above models do not include the flexibilities of the blades which may be important in many cases of full scale blades (as opposed to experimental blades which are relatively stiff). Moreover, in the axial flight region, the above approximate models are concentrated on the prediction of integral quantities (averaged induced velocity, rigid flap angle, and thrust). Thus, time-dependent development of the induced velocity distribution along the span is not dealt with. Knowing this distribution is essential for a realistic evaluation of the lift distribution as required during the

determination of elastic blades response.

From a structural point of view, the literature contains various models that are capable of representing the structural mechanism of elastic blades (see Ref. 1). In the present case of sharp changes in time, adoption of the finite-element approach seems to be inevitable due to the need to enable a time dependent simulation of dynamic response which contains a vast range of *a priori* unknown frequencies that depend on the shape and rate of the specific command.

The task of the present model is to formulate an approximate analytical model which will be capable of simulating the time history of the spanwise distribution of the induced velocity and the structural dynamic response of elastic blades and the rotor/fuselage system. The proposed mathematical formulation is capable of examining a variety of phenomena imposed by a rapid collective increase in hover and, therefore, provides a better insight into the involved physical mechanism.

## Analysis

### The Aerodynamic Loads

The present formulation is based on separating the problem into two regions: the "external field" and the "internal field". This separation is based on the traditional description of the flow-field mechanisms by discrete vortex lines. From this point of view, it is possible to show that a substantial part of the induced velocity over the blade is contributed by the trailing vortices which are created by the spanwise variations of the bound circulation. These vortices are located at all times in the blade's vicinity and their influence is three-dimensional (i.e. vortices which are shed from a certain cross-section induce velocity over other cross-sections and over other blades as well). Thus, the trailing vortices are suitable to be considered as the external field in which the interaction between the blades and their wakes is also taken into account. The influence of the trailing vortices is determined by a first order extension of the classical "blade-element-momentum" theory which is based on the vortex theory.

The shed vortices which are created by the time variations of the bound circulation are characterized, in contrast with the trailing vortices, by relatively short influence distances and are therefore suitable to be taken into account by two-dimensional considerations as the internal field. Thus, an unsteady two-dimensional analysis is carried out in the internal field for each cross-section along the blade span. For that purpose, the formulation presented by Dinyavari and Friedmann [10] is adopted. This formulation enables the calculation of the loads using two state variables which are

obtained by the time history of the normal velocity at the three-quarter-chord point. This velocity contains also the velocity induced by the trailing vortices of the external field, while the shed vortices are consistently included in the loads expressions.

**External field formulation:** As mentioned above, the present analysis is based on the extension of the classical "blade-element-momentum" theory (e.g. Ref. [1]). By momentum considerations for a control volume,  $V$ , which is defined by a ring in the rotor disc and the stream lines that pass along its internal and external circumference, it is possible to express the thrust vector generated over the ring's area in the disc plane as:

$$\bar{T} = \frac{\partial}{\partial t} \iiint_V \rho \bar{u} dV + \iint_S \bar{u} (\rho \bar{u} \cdot \hat{n} dS) \quad (1)$$

where  $\rho$  is the fluid density,  $\bar{u}$  is the velocity vector at each point in the control volume,  $t$  stands for time,  $n$  is a unit vector normal to the control volume surface (positive when directed outside), and  $S$  is the control volume surface. Clearly, the steady momentum theory does not account for the first term in Eq. (1). As shown in Ref. [1], it is possible to write the steady contribution of the control volume (based on the second term in Eq. (1)) as:

$$dT_M = 4\pi r v (V_c + v) dr \quad (2)$$

where  $dT_M$  is the thrust over a ring of width  $dr$  located at  $r$  (positive when directed upwards),  $v$  is the induced velocity at  $r$  (positive when directed downwards), and  $V_c$  is the rotor climb velocity (positive when directed upwards).

At this stage, the introduction of the first (unsteady) term in Eq. (1) to the analysis is studied. It is clear that the above mentioned unsteady term represents thrust that has been created by accelerating the air around the disc and, therefore, its contribution might be significant where sharp changes in thrust take place. In addition, it is clear that the air is accelerated differently at various locations in the disc vicinity. On top of that, representing the flow-field around the disc by vortex filaments shows that it is impossible to consider each ring separately (as opposed to the steady case for large enough numbers of blades - see Ref. [11]). Also, the classical assumptions of the momentum theory that led to Eq. (2) are not necessarily justified in this unsteady case.

In order to develop the present approximation it was assumed that there is a time-independent constant, that relates the rate of induced velocity change at a certain radial location over the disc to

the unsteady part of the thrust per unit length created at the same location. Consequently, it is possible to formulate the contribution of each ring to the overall thrust by:

$$\frac{dT_M}{dr} = 4\pi r v (V_c + v) + m(r) \dot{v} \quad (3)$$

where  $m$  will be referred to as the "equivalent mass" and is assumed to be a function of the ring's radial location,  $r$ , only and has a dimension of mass per unit length. As shown, the unsteady part has not been changed (see Eq. (2)). Note that this expression is similar to the classical "global" expression given in Ref. [5] which associates the overall induced velocity and the thrust. Once the assumption made in Eq. (3) is proven to be appropriate, it has the following advantages:

- It associates the induced velocity of each ring with its own thrust only.
- It enables clear identification of the unsteady and steady contributions and therefore may be reduced directly to the steady case.
- It preserves the basic structure of the exact equation (Eq. (1)).

The physical definition of the "equivalent mass" emerges directly from Eq. (3) as: **The mass that has to be accelerated, at each unit length, by the rate of change of the induced velocity over the corresponding ring in the disc plane, in order to obtain a thrust force per unit length which is equal to the one that is created by the nonuniform acceleration of the air over the entire control volume.**

It should be emphasized that the most critical assumption made in Eq. (3) is that  $m(r)$  is not a function of time which also states that it is independent of the command shape (or the circulation history). The justification of the above assumptions and the determination of  $m(r)$  are dealt with in what follows.

As a stage it is possible to examine in what way the above mentioned equivalent mass appears in the aerodynamic load expressions. First, the thrust created by a bound vortex element is given by:

$$dT_e = \rho \Omega r \Gamma dr \quad (4)$$

where  $dT_e$  is a thrust element,  $\Omega$  is the rotor angular velocity,  $b$  is the number of blades, and  $\Gamma$  is the bound vortex at radius  $r$ .

Equating Eqs. (3), (4) gives:

$$4\pi r v (V_c + v) + m \dot{v} = \Omega r \Gamma b \quad (5)$$

On the other hand, the bound vortex strength as a function of the time-dependent induced velocity may

be determined by any, either steady or unsteady, two-dimensional airfoil theory. For example, in the simplest case of the steady blade-element strip theory,  $\Gamma$  is given by:

$$\Gamma = \frac{1}{2}\Omega r c a \left[ \theta - \frac{v}{\Omega r} \right] \quad (6)$$

where  $a$  is the lift curve slope,  $c$  is the blade chord, and  $\theta$  is the blade local pitch angle.

Combining Eq. (5) with Eq. (6) by eliminating  $\Gamma$ , yields an equation where the unknowns are  $v(r,t)$  and  $m(r)$ . Clearly, in the steady case, this equation defines  $v(r)$ , however, additional information is required in the unsteady case. This information can not be obtained from the momentum theory or from the blade-element theory or from their combination, however, it may be acquired from the combination of the vortex theory with the momentum theory. Therefore, a consistent way for determining  $m(r)$ , which is based on the vortex theory, is dealt with next. Then a sensitivity study of  $m(r)$  will be presented.

In order to calculate the time changes in the induced velocity while using the vortex theory, a time stepping numerical scheme should be adopted so that the induced velocity over each cross-section may be calculated at each moment (by integrating the wake vortices influence according to Biot-Savart law). Using this velocity, the vorticity that generates vortex elements which are added in each time step to the flow-field is calculated and all other elements in the flow-field are "shifted" properly.

For the sake of clarification, it will be assumed that such a scheme has been applied to a given  $\Gamma(r,t)$ , the corresponding values of the induced velocity  $\bar{v}_V(r,t)$  were obtained, and it is desired to find the appropriate values of  $m(r)$ . Assuming that the induced velocity at the beginning of the process is  $v_0$ , Eqs. (5) and (6) may be integrated in the following form:

$$v = \frac{1}{m} \int_0^t \left[ \frac{1}{2} b \Omega^2 r^2 c a \left[ \theta - \frac{v}{\Omega r} \right] - 4\pi r v \left[ V_c + v \right] \right] dt + v_0 \quad (7)$$

Now, it is possible to set the requirement that the sum of the squares of the discrepancies between the induced velocity which is obtained from Eq. (7) and that which is obtained by the vortex theory will be minimal along a given time interval  $t_0$ , namely:

$$\text{minimize over } m \int_0^{t_0} \left[ v - \bar{v}_V \right]^2 dt \quad (8)$$

The values of  $m(r)$  are obtained from the above minimization which is carried out for each cross-

section. As will be shown in the following study,  $m(r)$  exhibits low sensitivity to most of the relevant parameters and, therefore, *a priori* values of  $m(r)$  may be used in many of the practical cases. Clearly, once  $m(r)$  is known, the induced velocity time history may be directly calculated by Eq. (5) for any given time dependent of circulation. Compared with the robust numerical vortex-theory scheme, the required computational effort is negligible in this case.

**Equivalent mass characteristics:** To demonstrate some characteristics of the above formulation, a numerical scheme based on the vortex theory is required. In the present paper, a helical wake model with varying spacings has been used. If needed, this model can be replaced by any other wake model. The output of this code is the distribution of the induced velocity at each moment as function of the blade span. In what follows, the results of a sequence of checks are presented. In these cases, the rotor is assumed not to produce thrust at  $t < 0$ . At  $t \geq 0$  thrust is starting to be created by various command shapes.

The purpose of the first check is to show that the value for the equivalent mass which has been obtained from the minimization process (Eq. (8)), permits the approximation of the induced velocity time history. The results of this check using a step increase of circulation are shown in Fig. 1. As shown, the development of the induced velocity as function of time which is obtained by using the above equivalent masses, gives a good approximation of the one which has been obtained by the vortex theory. Using these values of the equivalent mass, the induced velocity development in the case of double step variation in circulation was examined and satisfactory correlation has been obtained.

The purpose of the next check is to find the sensitivity of the equivalent mass values to the command shape characteristics. Consequently, the mass values which were obtained by different time histories of bound circulation initiated from zero at  $t=0$  and terminated at the same final value were examined - see Fig. 2. Generally, it may be stated that the equivalent mass distribution exhibits only low sensitivity to the command shape characteristics.

Next, the sensitivity of the equivalent mass to changes in the rotor's number of blades is studied. Figure 3 shows that the spanwise distribution of the equivalent mass becomes sharper as the number of blades is decreased. Thus, it may be concluded that for rotors having three blades or more, the number of blades has only a limited influence on the equivalent mass values and an asymptotic convergence is obtained as this number of blades is increased. It should be noted that integrating the distributed mass along the blade span for the case of a large number of blades, yields a value which is larger than the value used in Ref. [4] for an impervious disc by 10%.

To study the influence of the values of the

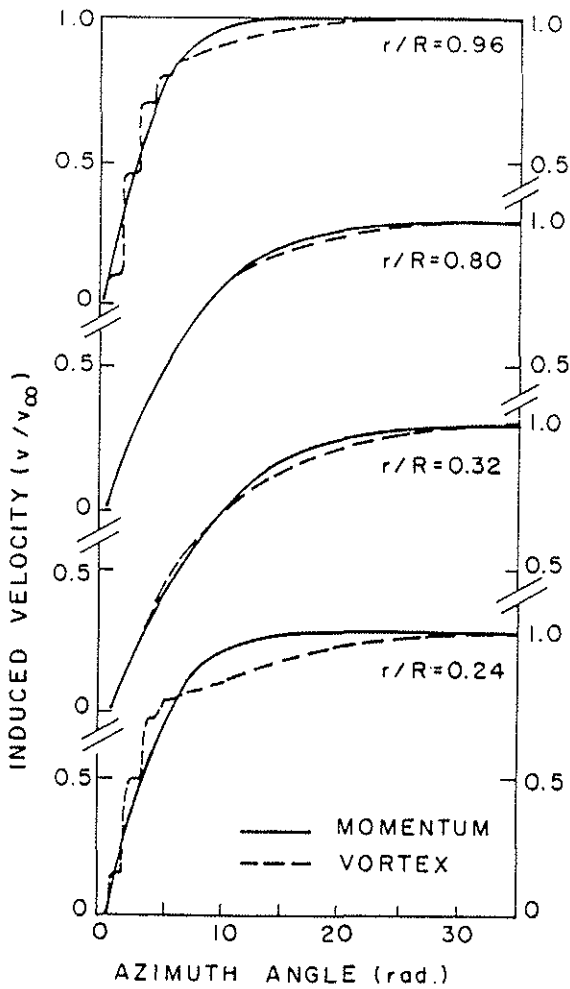


Fig. 1: Induced velocity development for a step function in circulation.

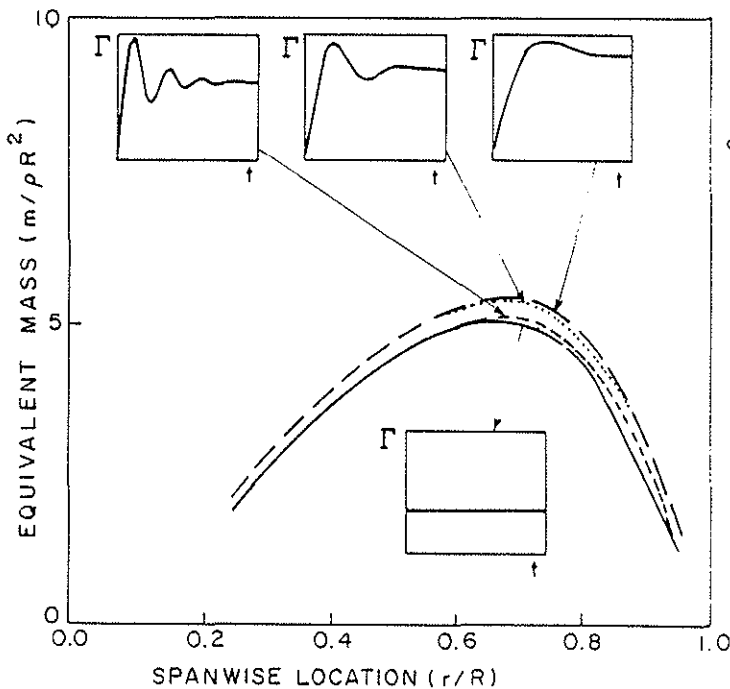


Fig. 2: Equivalent mass values for different command shapes.

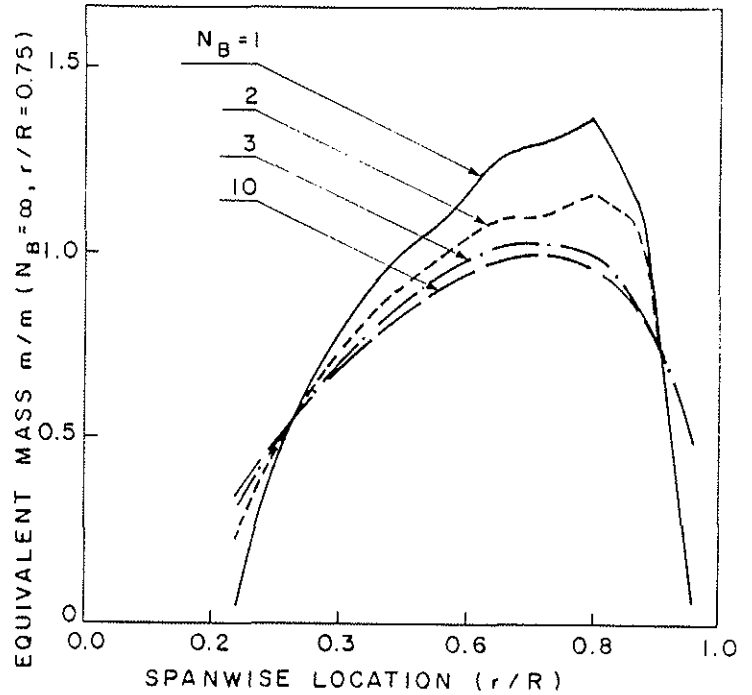


Fig. 3: Equivalent mass values for a different number of blades.

induced velocity and the bound vorticity at the starting moment ( $t=0$ ), the circulation end values of a number of step function commands were kept constant while the initial values were 0%, 17%, 33%, 50% and 67% of the end value. The results are presented in Fig. 4. As shown, the mass values increase

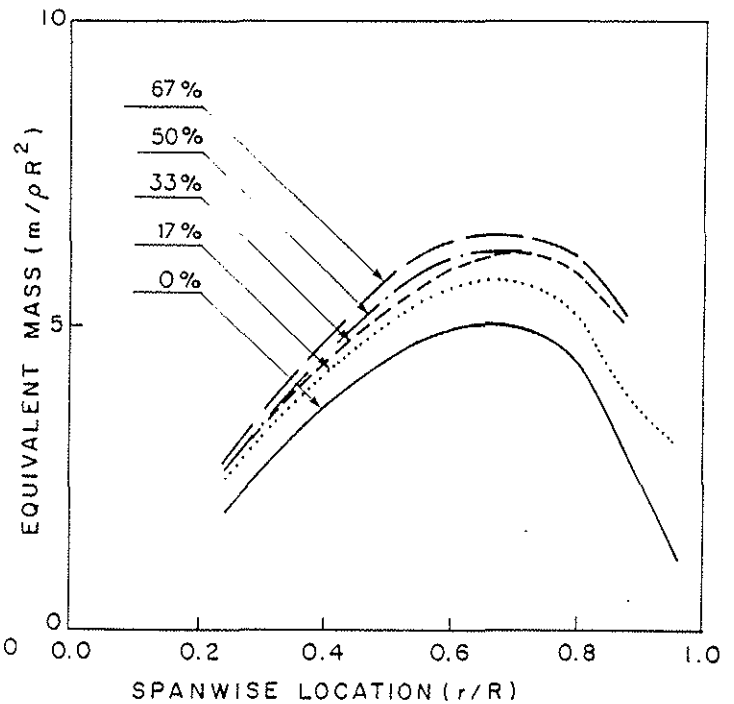


Fig. 4: Equivalent mass values for different initial values of circulation.

with the initial values. In addition, there is a lower bound for the mass values (the case of zero initial condition). From the vortex theory point of view, this phenomenon may be explained by the following argument: as the initial induced velocity is increased, the vortex segments are floating downstream away from the disc with higher velocity and create a larger angle relative to the disc plane. Thus, the mechanism that converts bound vorticity changes to induced velocity becomes slower which is equivalent to higher mass values. The conclusions drawn from this check is that the influence of the initial conditions is significant, however, it is bounded between well defined limits.

Study of the equivalent mass sensitivity to other parameters such as the end values of circulation and the spanwise load distributions may be found in Ref. 13.

### Equations of Motion

**System of coordinates:** As already mentioned, the present analysis deals with the response of a helicopter in hover and axial flight. Thus, it is convenient to choose a "Fuselage" system of coordinates  $(x_F, y_F, z_F)$  which is rigidly connected to the fuselage and parallel to the "Inertial" system  $(x_I, y_I, z_I)$  as shown in Fig. 5. The "Hub" system of coordinates  $(\hat{x}_H, \hat{y}_H, \hat{z}_H)$  is connected to the rotor at the hub and rotates with it. Figure 5 also defines the azimuth angle,  $\psi$ . In addition, a local "Deformed" system of coordinates  $(\hat{x}_D, \hat{y}_D, \hat{z}_D)$  is attached to each cross-section along the blade while its orientation is determined by the three rotations in the lead-lag,

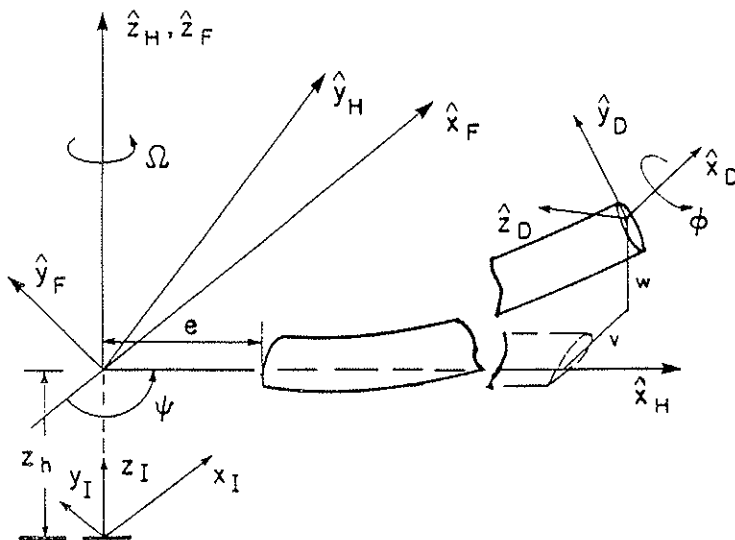


Fig. 5: The inertial, fuselage, Hub and deformed systems of coordinates.

flap and torsion directions, respectively.

**Degrees of freedom:** The present formulation includes elastic and rigid body degrees of freedom. The elastic degrees of freedom are the displacement in the flapwise direction ( $w$ ), and its spanwise derivative ( $w_x$ ), the displacement in the edgewise direction ( $v$ ), and its spanwise derivative ( $v_x$ ), and the elastic twist,  $\phi$ , about the elastic axis (after the transverse displacements took place). The helicopter rigid body degrees of freedom are the rotor's azimuth angle,  $\psi$ , and the vertical position of its center of gravity,  $z_h$  (see Fig. 5). Since no axial degree of freedom is included, an approximation of the radial motion due to the transverse displacements is utilized.

**The structural modeling:** From a structural point of view the blades are modeled as slender beams having arbitrary distributions of properties such as stiffness, mass, center of gravity location, etc. By adopting the Bernoulli-Euler assumptions and assuming small strains and moderate elastic rotations, the elastic rotations  $v_x$ ,  $w_x$  and  $\phi$  are defined as three Euler angles. To provide consistency of the trigonometric expressions of the above angles, the analytical derivation was based on a second order approximation for small angles.

**Position vector:** The derivation of the equations of motion is based on the expressions for the position vector of each material point of the blade (located at  $x, y, z$  in the  $\hat{x}_H, \hat{y}_H, \hat{z}_H$  directions before the deformation), in the inertial system, as a function of time:

$$\bar{R}_{(x,y,z,t)} = [T_{FH}] \left\{ \begin{Bmatrix} e \\ 0 \\ 0 \end{Bmatrix} + \begin{Bmatrix} X_e \end{Bmatrix} + [T_{HD}] \begin{Bmatrix} 0 \\ y \\ z \end{Bmatrix} \right\} + \begin{Bmatrix} 0 \\ 0 \\ z_h \end{Bmatrix} \quad (9)$$

where  $[T_{FH}]$  is a transformation matrix that transforms a vector in the Hub system to its form in the Fuselage system,  $e$  is the blade offset (see Fig. 5),  $\{X_e\}$  contains the elastic axis coordinates in the Hub system,  $y$  and  $z$  are the coordinates of a material point in each cross section,  $[T_{HD}]$  is a transformation matrix that transforms a vector in the Deformed system to its form in the Hub system, and  $z_h$  is the vertical position vector (height) of the hub.

Proper differentiation of the position vector with respect to time enables to express the kinetic energy and its derivatives as required for constructing the Lagrange equations of motion. It is important to note that all terms containing time

derivatives were retained in these equations. This is essential in the present case of rapid time variations where time derivatives may change their order of magnitude throughout the response. All analytical derivations were executed and coded using symbolic mathematical manipulation software [12].

**The finite-element formulation:** As already mentioned, the present solution is based on the finite-element approach. Accordingly, the blade is divided into beam elements. For each element, the following vector of degrees of freedom has been assigned:

$$\{q_X\} = \langle w_L, w_{xL}, v_L, v_{xL}, \phi_L, w_R, w_{xR}, v_R, v_{xR}, \phi_R \rangle^T \quad (10)$$

where the indices L and R stand for the element's left and right sides, respectively.

### Time Integration

Assembling the contributions of all the elements results in a coupled system of equations which is replaced by two equivalent systems of equations so that a separation between the rigid and the elastic degrees of freedom is obtained. Consequently, the resulting equations of motion become:

$$\begin{aligned} [M_{XX}] \{\ddot{q}_X\} + [K_{XX}] \{q_X\} + [C_X] \{\dot{q}_X\} + \{N_X\} \\ + [M_{XR}] \{\ddot{q}_R\} = \{Q_X\} \end{aligned} \quad (11a)$$

$$\begin{aligned} [M_{RR}] \{\ddot{q}_R\} + [K_{RR}] \{q_R\} + [C_R] \{\dot{q}_R\} + \{N_R\} \\ + [M_{XR}]^T \{\ddot{q}_X\} = \{Q_R\} \end{aligned} \quad (11b)$$

where  $[M_{IJ}]$ ,  $[K_{IJ}]$ ,  $[C_I]$ ,  $[N_I]$  are mass matrices, stiffness matrices, damping matrices, and vectors of nonlinear contributions, respectively.  $\{q_R\}$  contains the rigid degrees of freedom and is given by:

$$\{q_R\}^T = \langle \psi, z_h \rangle \quad (12)$$

Each time step in the simulation is carried out as follows:

- \* Initial values for  $\{q_X\}$ ,  $\{\dot{q}_X\}$ ,  $\{q_R\}$ ,  $\{\dot{q}_R\}$  are introduced.
- \* The time dependent terms in Eqs. (11a,b) are determined.
- \* The vector  $\{\ddot{q}_R\}$  is determined by Eq. (11b).
- \* The vector  $\{\ddot{q}_R\}$  is substituted in Eq. (11a) from which the vector  $\{\ddot{q}_X\}$  is obtained.
- \* Since nonlinear expressions are involved, the above steps are repeated until convergence is achieved.

Once the values of  $\{\ddot{q}_R\}$ ,  $\{\ddot{q}_X\}$  are obtained and an integration step is performed, the above iterative procedure is repeated for the next time step.

## Results

Based on the above aerodynamic model and the structural dynamic analysis, a code that simulates the time history of the involved degrees of freedom has been developed. The following is a summary of the parametric investigation and is based on a detailed description of the nominal case followed by successive variations of the main parameters. A full description of the above study may be found in Ref. 13.

### The Nominal Case

The nominal case is based on a typical full scale hingeless rotor-fuselage system, (see Ref. 13). The blades have uniform distribution of geometrical mass and stiffness properties and linear aerodynamic washout. Collective increase has been introduced by a "ramp" command (of 200 /sec) up to a constant value of 2. In addition, in this nominal case, the helicopter is not allowed to move vertically (i.e.  $z_h=0$ ).

**The flapping response:** This elastic motion is shown in Fig. 6 for the tip cross-section. Generally, this response consists of three main phases: A very short period where almost no response is observed, a period which includes a definite upraising of the flapping motion and an overshoot (of about 62%), and a third period where the system settles down towards a steady-state position while having highly damped small oscillations.

**The lead-lag response:** This elastic motion is also presented in Fig. 6. As shown, the response does not exhibit an overshoot and is mainly characterized by oscillatory motion having low damping. In this nominal case, the motion is mainly the result of the distribution of the aerodynamic inplane loads.

**The twist response:** Since the nominal case contains almost no aerodynamic torsional moment (due to the coincidence of the elastic axis and the aerodynamic center and the absence of pure aerodynamic

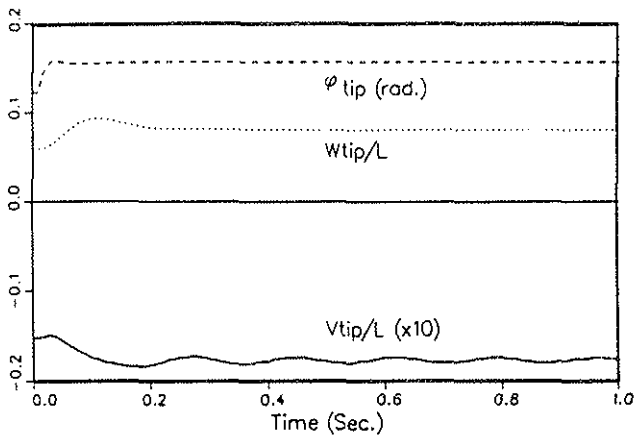


Fig. 6: The elastic flap, lead-lag and twist tip response (nominal case).

moment), the resulting twist angle shown in Fig. 6, is caused mainly by the torsional dynamics induced by the root torsional moment and small unsteady contributions of the aerodynamic moment.

**The induced velocity response:** As shown by the full lines in Fig. 7, in the outboard sections the development of the induced velocity with time is characterized by a small lag at the beginning of the motion, followed by a notable raising. Then, the induced velocity is slowly decreased towards a steady state value. On the other hand, the values in the in-board sections reach their steady state by monotonic asymptotic approach. The lag of the induced velocity at the beginning is caused by a temporary decrease in the aerodynamic loads due to the rapid development of the flapping motion (Fig. 6), and the change in pitch rate at the end of the command "ramp". The induced velocity response for slower command rates will be discussed later.

**The thrust response:** Figure 8a describes the rotor aerodynamic thrust response (by a full line).

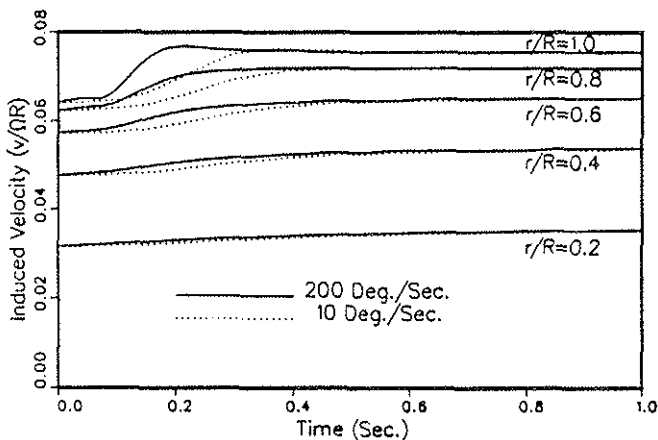


Fig. 7: The induced velocity response for 200°/sec (nominal case) and for 10°/sec.

As shown, the first peak has a "pointed" shape, then a sharp minimum is observed followed by a second overshoot peak (of 42%), while the thrust at steady-state is 34% higher than the initial one. Similar behavior may be found in Ref. [2] which is based on a vortex theory numerical scheme. Note that the aerodynamic thrust is obtained by integrating the aerodynamic loads along the blades span in the  $z_H$  direction and is only part of the total thrust that is transferred to the fuselage. Figure 8a also presents (by a dotted line) the total thrust acting on the fuselage which also includes dynamic loads. Comparison of the total and the aerodynamic thrusts demonstrates the important role of the dynamic response and reveals some interesting facts. First, the pointed peaks in the aerodynamic thrust has disappeared. Moreover, there is some lag in the total thrust at the initial response as opposed to a sharp rise of the aerodynamic thrust at that time. In addition, the total thrust is growing rapidly after this lag and reaches higher values than that of the aerodynamic thrust and in shorter time. These phenomena are the result of the elastic flapping motion which exhibits high acceleration and velocity values at the region under discussion. The blade mass which is accelerated upwards, results in a downward force acting on the fuselage. This force is subtracted from the aerodynamic thrust and since its magnitude is almost equal to the aerodynamic force at the very beginning, the resulting load is very small. Following this initial response, the flapping motion is decelerated and the total thrust increases rapidly. The above phenomena is even more pronounced in the case of articulated blades.

**The axis moment:** Prior to the introduction of the collective pitch change, the axis moment in the  $z_H$  direction which is required for sustaining the rotational speed is determined. Then, assuming that during the blades' response the rotational speed remains constant, Fig. 8b presents (by the full line) the additional (negative) aerodynamic axis moment which is required to maintain the rotation. In contrast to the thrust behavior, this response has relatively low overshoot (6%). This phenomenon results from the in-plane aerodynamic loads and in particular the induced drag which depends on aerodynamic lift. Downward flapping results in an increase in the angle of attack that also rotates the lift vector forward so that its in-plane components contribute to a decrease in the required moment. Figure 8b also presents (by the dotted line) the additional total moment needed for maintaining constant angular speed. As shown the total moment response is different from the aerodynamic moment response and reflects some oscillations induced by the lead-lag motion. This behavior is a result of Coriolis loads which are created by the inward motion of the blade towards the rotation axis due to the

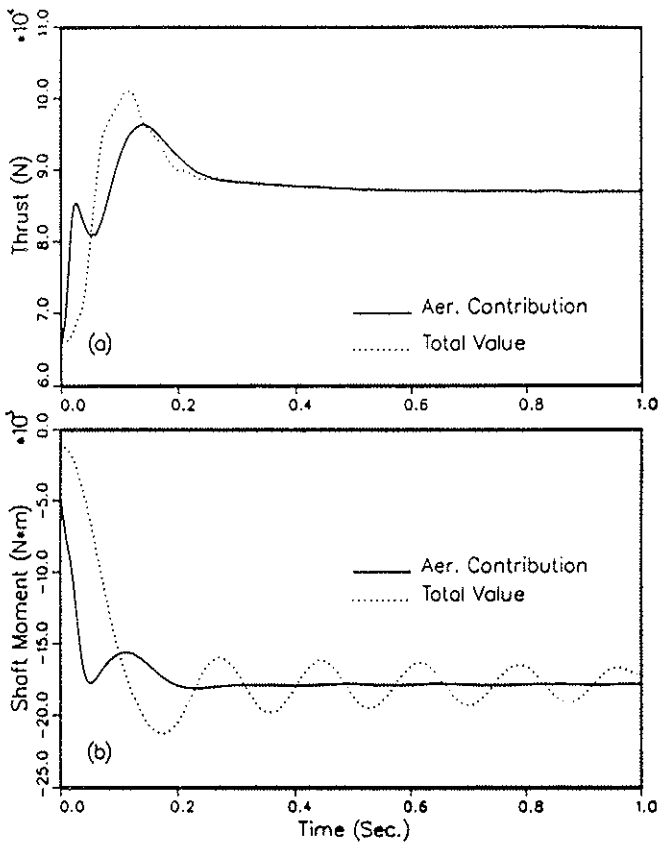


Fig. 8a,b: The response of the aerodynamic contributions and the total values of the thrust and shaft moment (nominal case).

flapping motion. These loads tend to reduce the required axis moment at the initial response and are even more dominant in the case of articulated blades.

**The root moments:** As shown in Fig. 9, the flapwise bending moment response is characterized by an

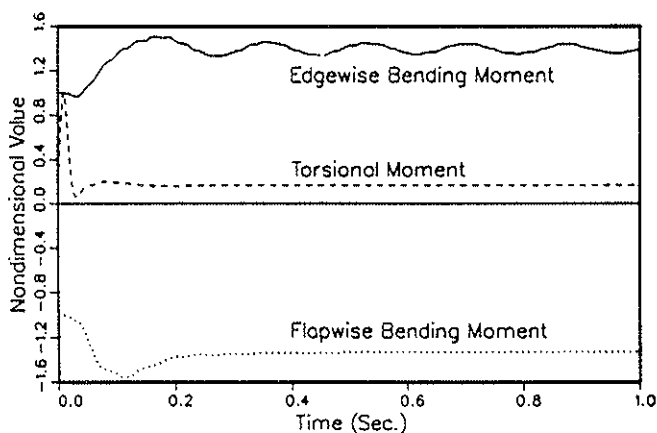


Fig. 9: The response of the root moments (nominal case). The flapwise and edgewise moments are normalized by their values at  $t=0$ . The torsional moment is normalized by its maximum value.

overshoot (of about 63%) and is similar to that of the flapping motion. In addition, like the lead-lag motion, the response of the resultant edgewise moment is characterized by an oscillatory motion of low damping and relatively small overshoot. The introduction of a "ramp" collective pitch command results in a substantial pitching acceleration of the blade's root at the beginning and at the end of the command. As shown in Fig. 9, the high value of torsional moment which is obtained at the beginning of the motion is highly damped and is immediately settled down to its steady state value. Note that in spite of the absence of aerodynamic torsional moment in the steady state position, there is some torsional moment along the blade which is a result of inertial contributions.

**The angle of attack and lift distribution:** The effective aerodynamic angle of attack shown in Fig. 10 is measured at the three-quarter chord location as required by the inner aerodynamic solution - see Ref. [10]. Note that this angle is the result of the blade's collective pitch and its rate, the flapping motion velocity and the helicopter climbing rate. As shown, the aerodynamic angle of attack responds relatively fast due to the high command rate that affects the angle of attack with no time delays. Subsequently, it is evident that the blade's flapping velocity dominates the response. Later on, due to the development of the induced velocity, the angle of attack is slowly decreased towards its steady state value.

### Sensitivity Study

In what follows, a summary of the parametric study is presented. In each case, the nominal case has been perpetuated by changing only one of the parameters.

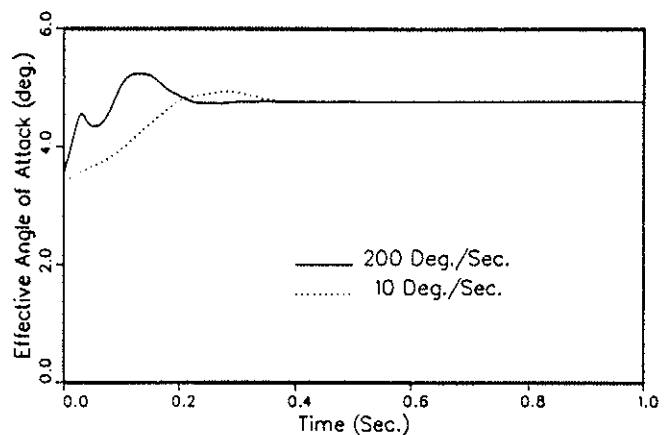


Fig. 10: The tip aerodynamic effective angle of attack response for  $200^\circ/\text{sec}$  (nominal case) and for  $10^\circ/\text{sec}$ .

**Command rate:** Different command rates have been examined from which it became obvious that this parameter has a notable influence. In the case of very slow command rate, the response of most of the parameters becomes almost monotonic having small overshoot and the pointed peak that has characterized the aerodynamic angle of attack and thrust has disappeared, as shown for the angle of attack by Fig. 10. In addition, in the case of slow command rate, the induced velocity development is characterized by an initial lag followed by almost linear increase until it settled down to a constant value - see Fig. 7. It should also be mentioned that increasing the command rate beyond 250 /sec cause almost no change in the induced velocity development, and as long as the aerodynamic response is considered, the command may be viewed as a step function.

**Climb rate:** In this case the helicopter vertical degree of freedom,  $z_h$ , has been released.

The results show that the climb rate increases almost linearly with time and the helicopter reaches a climbing velocity of 2.5 m/sec within one second. The response of all other parameters in this case, including the induced velocity and the thrust, exhibits lower steady-state values due to the decrease in the effective angle of attack that is caused by the climbing velocity. However, the overshoot values are basically unchanged since the climb velocity reaches influential values only after most of the transient phenomena are over. Note that this phenomenon depends on the fuselage weight and excessive small values of it may cause significant changes in the above described response.

**The rotational speed variations:** A number of values for the motor moment of inertia were examined (note that infinite value is used in the nominal case). As shown in Fig. 11, the rotational speed decrease is very slow and therefore, similar to the

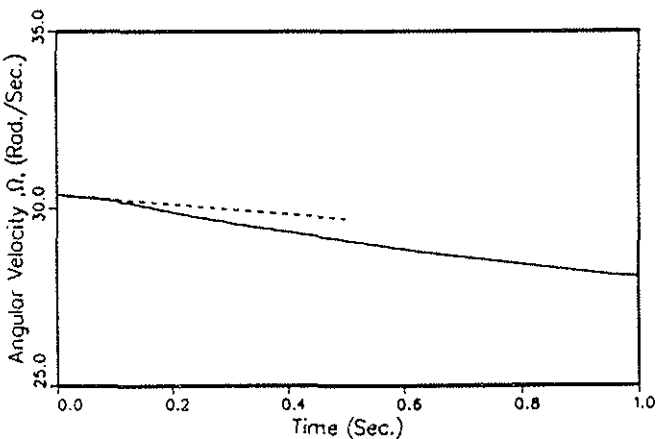


Fig. 11: The rotational speed response for finite value of the motor moment of inertia.

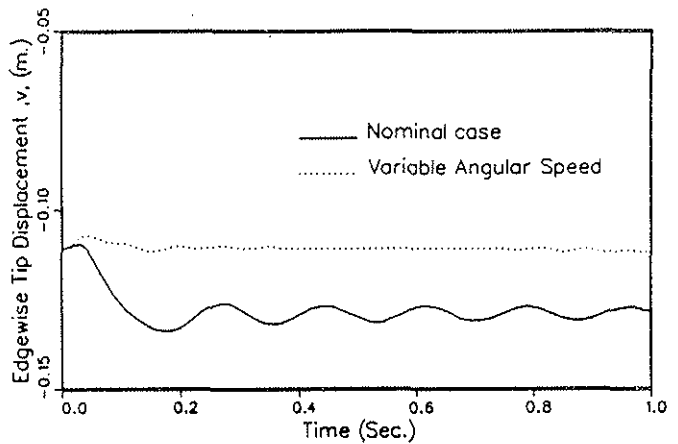


Fig. 12: The lead-lag response for finite value of the motor moment of inertia.

climb rate, its influence is experienced only after the overshoot region as monotonic and slow decrease in most of the parameters (lift, deformations, etc.). The rotational speed decreases more rapidly as the motor moment of inertia becomes smaller up to the theoretical limit where the rotor moment of inertia becomes dominant. The relatively small lag in the initial rotational speed decrease which is stressed by the dashed line in Fig. 11, results from the mechanism described above for the shaft moment behavior - see Fig. 8b. Also, the lead-lag motion is highly influenced by the changes in the motor moment of inertia and as shown in Fig. 12, the rotational speed variation introduces some damping to this motion by allowing the motor to "absorb" some of the vibrational lead-lag loads.

**The torsional stiffness:** Figure 13 presents the aerodynamic thrust response for two different values of torsional stiffness of the blades - a half value and a double value of the nominal case, respectively. As shown, the torsional stiffness has a crucial influence on the pointed peak phenomena mentioned

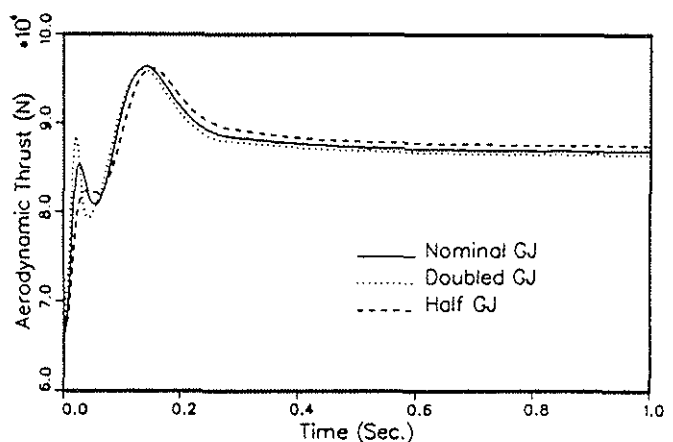


Fig. 13: The aerodynamic thrust response for different torsional stiffnesses.

above with regard to the aerodynamic thrust, lift and angle of attack behavior. However, the second overshoot is not sensitive.

**The aerodynamic equivalent mass:** Figures 14 and 15 present the induced velocity and thrust response, respectively, for vanishing values for the aerodynamic equivalent mass which represents no lag in the development of the trailing wake induced velocity. Note that the inner aerodynamic field still contains some unsteady effects. As shown, the induced velocity response is much more oscillatory in this case. Also, comparison of Figs. 8a and 15 shows that although oscillatory motion is observed for vanishing values of the equivalent mass, the total thrust overshoot has not been changed.

### Experimental Correlation

Correlations with experimental results presented by Carpenter and Fridovich [4] are presented

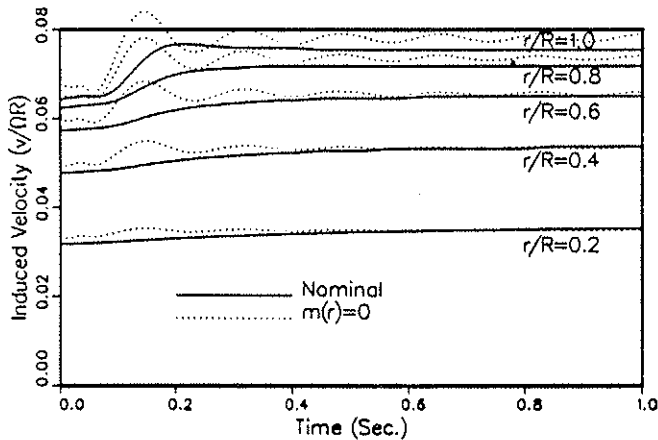


Fig. 14: The induced velocity response for vanishing equivalent mass values.

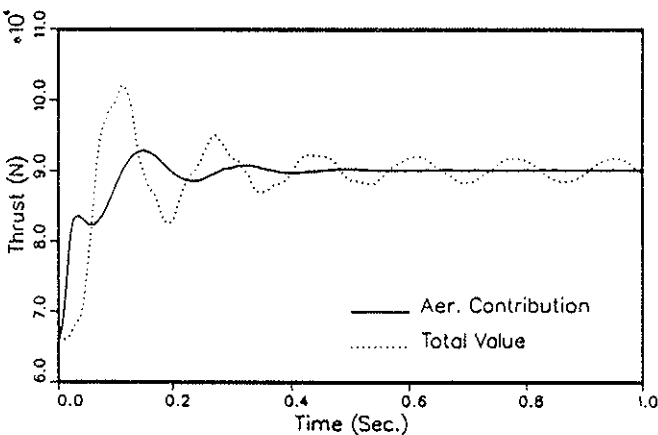


Fig. 15: The aerodynamic and total thrust response for vanishing equivalent mass values.

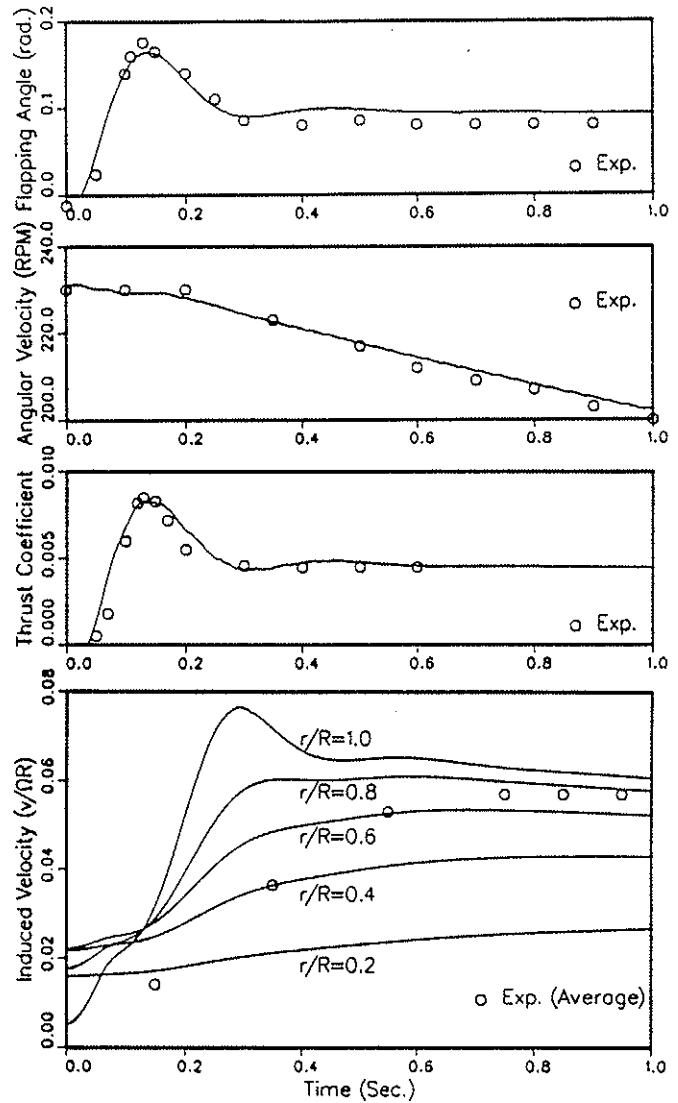


Fig. 16: Correlation with experimental data of Ref. [4] for articulated rotor.

in Fig. 16. In these experiments, articulated blades undergoing rapid variations in collective pitch angles were tested. Note that there are some uncertainties in the data concerning blade properties (center of gravity and aerodynamic center location, stiffnesses, etc.). Overall, the results presented in Fig. 16 for command rate of  $200^\circ/\text{sec}$  demonstrate good correlation. The lag in the rotational speed decreases at the initial response is clearly observed in this case. It should also be pointed out that the measured induced velocity represents an average value.

### Concluding Remarks

Theoretical study of the response of helicopter blades to a sharp collective change in hover has been presented.

The three-dimensional, unsteady aerodynamic solution is based on the definition and determination of the distribution of equivalent aerodynamic mass.

Parametric study has proved that this mass distribution has low sensitivity to most of the involved parameters and *a priori* determination of it is justified. The usage of these equivalent mass values for the calculation of the induced velocity response enables substantial saving of computational effort.

Combining the aerodynamic modeling with structural dynamic analysis of elastic blade, yielded some interesting observations:

- (a) In cases of rapid collective increase, the response is dominated by the dynamics of the elastic flapping motion which also creates notable differences between the aerodynamic thrust and the total thrust transferred to the fuselage.
- (b) There is a lag in the development of the required shaft moment response due to the rapid flapping response.
- (c) The command rate has a significant influence on the overshoot values of most parameters.
- (d) The equivalent mass was found to play an important role. However, the results' sensitivity to small changes in its values was found to be smaller in cases of rapid collective change since the induced velocity development is relatively slow and becomes influential only after the flapping motion has reached its maximal values.
- (e) Elastic effects were found to be important in hingeless blades due to their crucial influence on aerodynamic loads. In particular, a pointed peak in the aerodynamic loads development is clearly observed in blades having high torsional stiffness and disappear in blades that are soft in torsion.

### References

1. Johnson, W., "Helicopter Theory", Princeton University Press, New Jersey, 1980.
2. Segel, L., "Air Loadings on a Rotor Blade as Caused by Transient Inputs of Collective Pitch", USAAVLABS Technical Report 65-65, Oct. 1965.
3. Chen, R.T.N., "A Survey of Nonuniform Inflow Models for Rotorcraft Flight Dynamics and Control Applications", 15th European Rotorcraft Forum, Amsterdam, The Netherlands, Sept. 12-15, 1989.
4. Bir, G. and Chopra, I., "Prediction of Blade Stresses Due to Gust Loading", Vertica, Vol. 10, No. 3/4, pp. 353-377, 1986.
5. Carpenter, P.J. and Fridovich, B., "Effects of a Rapid Blade-Pitch Increase on the Thrust and Induced Velocity Response for a Full-Scale Helicopter Rotor", NACA TN 3044, Nov. 1953.

6. Rebont, J., Valensi, J. and Soulez-Lariviere, J., "Response of a Helicopter Rotor to an Increase in Collective Pitch for the Case of Vertical Flight", NASA Technical Translation F-55, June 1959.
7. Pitt, D.M. and Peters, D.A., "Theoretical Prediction of Dynamic-Inflow Derivatives", Vertica, Vol. 5, pp. 21-34, 1981.
8. Chen, R.T.N. and Hindson, W.S., "Influence of Dynamic Inflow on the Helicopter Vertical Response", Vertica, Vol. 11, No. 1/2, pp. 77-91, 1981.
9. Houston, S.S. and Tartelin, P.C., "Validation of Mathematical Simulation of Helicopter Vertical Response Characteristics in Hover", Journal of the American Helicopter Society, Vol. 36, No. 1, pp. 45-57, 1991.
10. Dinyavari, M.A.H. and Friedmann, P.P., "Unsteady Aerodynamics in Time and Frequency Domains for Finite Time Arbitrary Motion of Rotary in Hover and Forward Flight", AIAA Paper 84-0988, 1984.
11. Rand, O. and Rosen, A., "Efficient Method for Calculating the Axial Velocities Induced Along Rotating Blades by Trailing Helical Vortices", J. of Aircraft, Vol. 21, No. 6, pp. 433-435, 1984.
12. Seward, L.R., "Reduce User's Guide for IBM 360 and Derivative Computers", Version 3.3, The Rand Corporation, Santa Monica, CA 90406, U.S.A., July 1987.
13. Hecht, Y., "Response of Helicopter Blades to a Sharp Collective Change", M.Sc. Thesis, 1990, Faculty of Aerospace Eng., Technion - I.I.T.